XI Congreso Nacional y II Internacional
de Ingeniería Termodinámica

11CNIT-29180-2019 FULLPAPER

# Theoretical comparison of the performance of two-stage reciprocating compressor, a two-stage scroll compressor, and a vapor-injection scroll compressor

Fernando M. Tello-Oquendo[1], Emilio Navarro-Peris[1], José Gonzálvez-Maciá[1]

[1]Universitat Politècnica de València, Instituto Universitario de Investigación en Ingeniería Energética, Camino de Vera s/n, Valencia, 46022, Spain, Phone: 34-96-3879120, Fax: 34-96-3879126
e-mail: fertelo1@upvnet.upv.es

## ABSTRACT

Vapor-injection technique comprises the injection of vapor refrigerant into an intermediate stage of compression. This technique is used in refrigeration systems and heat pumps working in extreme conditions. The advantages of vapor-injection are the improvement of capacity and COP in severe climates and the reduction of the compressor discharge temperature. The vapor-injection scroll compressor (SCVI) is one of the most frequently used compressors in heat pump systems with vapor-injection technique. In this case, the refrigerant is injected during the compression process into the scroll chambers. The intermediate pressure and refrigerant flow depend on the compressor design and the injection port size and location. Another common compressor technology with vapor injection is the two-stage reciprocating compressor (TSRC). In this case, the vapor-injection is performed after the first stage of compression. Therefore, the refrigerant discharged for the first stage of compression is mixed with the injection refrigerant before entering the second-stage compressor. The advantage of the scroll technology is the high volumetric efficiency for all compressor-working envelope, and it has a good compressor efficiency for moderate pressure ratios (< 7). On the other hand, the reciprocating compressors have a flatter compressor efficiency curve, but the volumetric efficiency rapidly decreases with the pressure ratio. Another possibility of the vapor-injection compressor is the two-stage scroll compressor (TSSC). Nevertheless, there is not a systematic evaluation of the performance of this compressor technology and a comparison with the previously described technologies.

This paper presents a performance comparison of three compressor technologies with vapor-injection, two-stage reciprocating compressor, two-stage scroll compressor, and vapor-injection scroll compressor. The comparison is performed in terms of the compressor efficiencies, discharge temperature, heating capacity, and COP. In order to do that, semi-empirical models of the compressors have been implemented for each compressor technology. The models consider the main sources of losses in the compression process and are able to predict the compressor efficiencies in terms of empirical parameters, which have a direct physical interpretation. Results show that SCVI presents better COP and efficiency with pressure ratios below 5; the TSSC and TSRC perform better with higher pressure ratios (above 7), nevertheless the TSSC present higher volumetric efficiency and heating capacity than the TSRC. The irreversibilities in the compression process of the TSSC decrease the compressor efficiency for low and moderate pressure ratios compared with the SCVI.

*Keywords*: *Compressor; Scroll; Reciprocating; Two-stage; Comparison; Semi-empirical model*

## 1. Introduction

Heat pumps working with a single-stage vapor compression cycle present several limitations when operating under extreme conditions, that is, low evaporating temperatures and high condensing temperatures. At high pressure ratios, the performance (COP) and capacity of the heat pumps decrease dramatically. Under these conditions, the compressor's isentropic and volumetric efficiencies significantly decrease, while the discharge temperature increases. In this context, the use of two-stage compression cycles with vapor-injection constitutes an effective solution to improve the performance of heat pumps and to extend the operating envelope of these systems. The vapor-injection technique improves the system capacity and COP and reduces the discharge temperature of the compressor [1].

The scroll compressor with vapor-injection (SCVI) is one of the most used compressor technology in two-stage cycles with vapor-injection. Numerous studies have been conducted using SCVI in heat pumps and refrigeration systems. Some of them analyzed the advantages of two-stage cycles with vapor-injection over single-stage cycles, other studies have focused on the control and optimization of the system and the use of different refrigerants in vapor-injection cycles are studied. Moreover, some studies have addressed the SCVI characterization methodologies and the SCVI modeling [2-8]. Nevertheless, scroll compressors have a fixed built-in volume ratio, which is determined by the scroll geometry. This produces over- and under-compression when the operating conditions deviate from the specified design condition. Therefore, the compressors can not work with the optimum efficiency when the operating pressure ratio differs from the design pressure ratio.

On the other hand, the two-stage reciprocating compressor (TSRC) is mainly used with vapor-injection in systems with two-stage compression. This compressor technology is used in applications with high pressure ratios. Tello-Oquendo et al. [9] conducted a comparison of two compressor technologies with vapor-injection, an SCVI and a two-stage reciprocating compressor (TSRC). The compressor performances were studied in a vapor-injection cycle with an economizer, using R-407C as refrigerant. The seasonal performances of both cooling and heating modes were estimated. The compressors comparison was conducted in terms of compressor efficiencies, COP, and heating capacity working in a wide range of operating conditions. Nevertheless, the catalog data of the TSRC were limited and it was not possible to predict the discharge temperature of this compressor. The TSRC model was based on efficiency curves and no comparison was made of the discharge temperature of the compressors.

Another possibility to improve the compression process is by using a two-stage scroll compressor (TSSC). This compressor consists of two scroll compressors arranged in series with vapor-injection between the two stages. A few studies have been developed about the application of the TSSC in heat pump systems. Kwon et al. [10] studied a heat pump with a TSSC for district heating using waste energy and R-134a as refrigerant. The authors analyzed the influence of the heat source temperature and the superheat at the low-stage compressor on heating capacity and COP. The COP improves by up to 22.6% when the heat source temperature is raised from 10 °C to 30 °C. Varying the frequency of the high-stage compressor to control the intermediate pressure results in a performance improvement of up to 5.2%. Bertsch and Groll [11] studied an air-source heat pump using a TSSC working with R-410A as refrigerant. The heat pump was tested at ambient temperatures as low as -30 °C to 10 °C and supply water temperatures of up to 50 °C in heating mode. The two-stage mode operation approximately doubles the heating capacity compared with the single-stage mode operation at the same ambient temperature. The discharge temperatures of each compression stage are kept below 105 °C, over the whole operating range.

Up to this point, a systematic comparison between an SCVI, a TSSC and a TSRC has not been addressed. The current paper addresses an evaluation of the performance of the three compressor technologies for heat pump applications, working under extreme conditions. Semi-empirical models of the three compressors are used in the study. The models are adjusted with experimental data collected in the laboratory. An SCVI, a non-injected scroll compressor (SCNI) and a reciprocating compressor (RC) were characterized in a calorimetric test bench, using R-290 as refrigerant. The systematic comparison of the performance of the three compressors is conducted in terms of compressor efficiencies, COP, heating capacity, and discharge temperature, in a wide range of operating conditions.

## 2. Methodology

### 2.1 Cycle model

Figure 1 depicts a general schematic of the two-stage vapor compression cycle and the P-h diagram. The cycle uses an internal heat exchanger (economizer) in the injection mechanism.

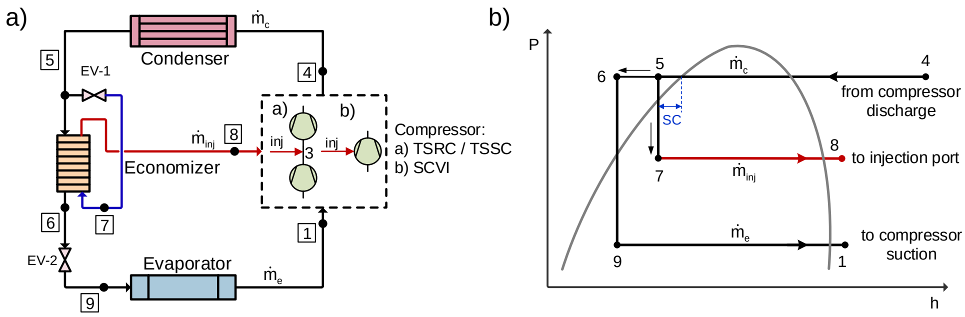


Figure 1. Two-stage vapor compression cycle with vapor-injection. a) Schematic of the cycle with an economizer. b) P-h diagram.

The pressure levels of the system ($P_1$, $P_4$, $P_8$) are calculated as the saturation pressures of the dew temperatures at the evaporator, condenser, and injection, respectively. The pressures of the points 5, 6, 7 and 9 are defined by introducing the assumption of null pressure drop in the lines and heat exchangers of the system. The enthalpies of points 7 and 9 are defined by introducing the assumption of isenthalpic expansion in the valves (see Figure 1b). The temperatures of points 1 and 5, and therefore their enthalpies, are calculated using the input parameters of superheat and subcooling. The energy balance of Equation (1) is met in the injection mechanism (economizer), and the condenser mass flow rate is defined by Equation (2).

$$\dot{m}_c h_5 = \dot{m}_e h_6 + \dot{m}_{inj} h_8 \tag{1}$$

$$\dot{m}_c = \dot{m}_e + \dot{m}_{inj} \tag{2}$$

The model parameters are the evaporating and condensing temperatures ($T_e$, $T_c$), suction superheat, injection superheat and subcooling at the condenser outlet (SH, $SH_{inj}$, SC). The compressor models, described below, calculate the evaporator mass flow rate, injection mass flow rate, compressor efficiencies, and discharge temperature. The output variables of the cycle model are heating capacity (Equation (3)) and heating COP (Equation (4)). The injection superheat is fixed to 5 K. The economizer size is fixed by setting a constant temperature approach of 5 K in the economizer ($T_6$ -$T_7$ in Figure 1a).

$$\dot{Q}_h = \dot{m}_c (h_4 - h_5) \tag{3}$$

$$COP_h = \frac{\dot{Q}_h}{\dot{E}} \tag{4}$$

In the present study, three types of compressors are considered. A scroll compressor with vapor-injection (SCVI), a two-stage reciprocating compressor (TSRC) and a two-stage scroll compressor (TSSC). Figure 2 illustrates the schematic of the compressor models. In the SCVI, the vapor-injection is performed at an intermediate pressure during the compression (see Figure

2a). In the TSRC and the TSSC, the vapor-injection is performed after the first stage of compression in a mixing chamber at constant pressure (see point 3 in Figure 2b). The point 3 is defined by Equation (5), assuming a perfect adiabatic mixing between the injection mass flow rate (point 8) and the evaporator mass flow rate (point 2).

$$\dot{m}_c h_3 = \dot{m}_e h_2 + \dot{m}_{inj} h_{inj} \tag{5}$$

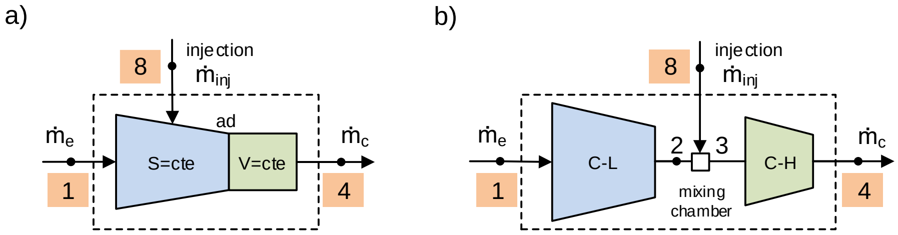


Figure 2. Model scheme of the vapor-injection compressors. a) SCVI. b) TSRC and TSSC.

The TSSC is composed of two non-injected scroll compressors (SCNI) arranged in series, with vapor-injection between the two compression stages. To model each SCNI, a semi-empirical model of scroll compressor was implemented according to Tello-Oquendo et al. [12] and [13]. This model was validated experimentally and can reproduce the compressor efficiency and the volumetric efficiency with a deviation lower than ±5% and ±3%, respectively. In addition, the model estimates the mass flow rate, the compressor power input and the discharge temperature with a deviation lower than ±3%, ±5%, and ±3 K, respectively [13].

Figure 3 shows the scheme of the refrigerant evolution through the compressor assumed in the model. The refrigerant enters the compressor at point 1 (suction) and leaves the compressor at point 2 (discharge).

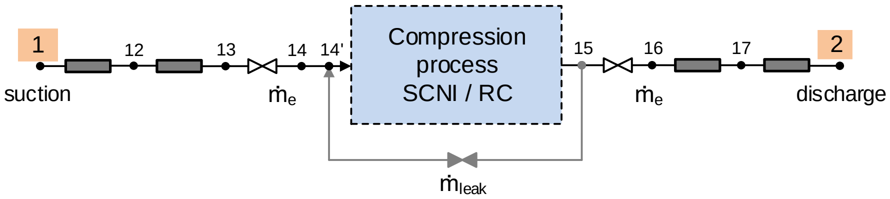


Figure 3. Model scheme of the refrigerant evolution inside the compressor, for non-injected scroll compressors (SCNI) and reciprocating compressors (RC).

The volumetric efficiency of the SCNI is calculated by Equation (6). The overall compressor efficiency is calculated by Equation (7), where $h_{2s}$ is the enthalpy at the discharge pressure considering an isentropic compression from the compressor inlet. The mass flow rate is calculated by Equation (8), where $\dot{V}_s$ is the swept volume of the compressor, $\rho_1$ is the density at the compressor inlet, and *n* represent the compressor speed.

$$\eta_v = \frac{\dot{m}_e}{\dot{V}_s\, \rho_1} \tag{6}$$

$$\eta_c = \frac{\dot{m}_e\,(h_{2s} - h_1)}{\dot{E}} \tag{7}$$

$$\dot{m}_e = \eta_v\, \dot{V}_s\, \rho_1 \tag{8}$$

Moreover, in order to define an overall compressor efficiency of the TSSC the Equation (9) is defined, where $h_{4s}$ represents the enthalpy at the discharge pressure of the high-stage compressor, considering an isentropic compression from the compressor inlet condition (point 3 in Figure 2b).

$$\eta_c = \frac{\dot{m}_e\,(h_{2s} - h_1) + \dot{m}_c\,(h_{4s} - h_3)}{\dot{E}_L + \dot{E}_H} \tag{9}$$

The SCVI was modeled as proposed by [13]. This semi-empirical model describes the vapor-injection into scroll compressors by using an empirical correlation (Equation (10)), which relates the injection ratio ($\dot{m}_{inj}/\dot{m}_e$) and the intermediate pressure ratio ($P_{int}/P_e$) (7). The correlation (10) allows estimating the injection mass flow rate as a function of the intermediate pressure for a given evaporation pressure level. The coefficients A and B are obtained by linear regression, based on the experimental data of the SCVI.

$$\frac{\dot{m}_{inj}}{\dot{m}_e} = A + B\,\frac{P_{int}}{P_e} \tag{10}$$

Figure 4 depicts the evolution of the refrigerant assumed in the SCVI model in a P-h diagram. The complex process of refrigerant injection is simplified as instantaneous isobaric mixing at the intermediate pressure. The reference for the compressor efficiency is given by an isentropic condition from the inlet to the outlet of the compressor ($4_s$) for the suction mass flow rate, and by an isentropic condition from the injection (inj) to the discharge pressure ($11_s$) for the injected mass flow rate. The real conditions at the compressor outlet are indicated by state 4 in Figure 4. The volumetric efficiency of SCVI is defined by the Equation (6). The overall compressor efficiency of SCVI is defined by Equation (11), where $h_{4s}$ represents the enthalpy at the compressor discharge pressure considering an isentropic compression from the compressor inlet pressure (point 1), and $h_{11s}$ represents the enthalpy at the compressor discharge pressure considering an isentropic compression from the intermediate pressure (point inj).

$$\eta_c = \frac{\dot{m}_e\,(h_{4s} - h_1) + \dot{m}_{inj}\,\left(h_{11s} - h_{inj}\right)}{\dot{E}} \tag{11}$$

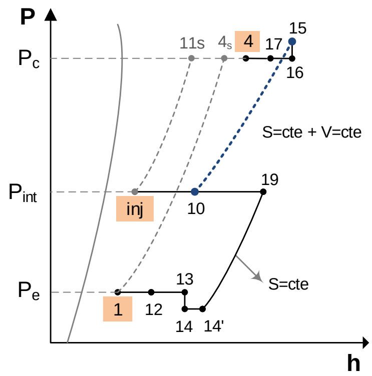


Figure 4. P-h diagram of the refrigerant evolution inside the vapor-injection scroll compressor.

The described model of the SCVI was validated experimentally and can reproduce the compressor efficiency and the volumetric efficiency with a deviation lower than ±5%. In addition, the model estimates the mass flow rate, the injection mass flow rate, the compressor power input and the discharge temperature with a deviation lower than ±2%, ±4%, ±5%, and ±4 K, respectively [13].

On the other hand, the TSRC is composed of two reciprocating compressors (RC) arranged in series, with vapor-injection between the two compression stages (see Figure 2b). In order to model the RC of each stage, a semi-empirical model was implemented according to Navarro-Peris et al. [14-15]. The model was validated experimentally and can reproduce the compressor efficiency and the volumetric efficiency with a deviation lower than ±4%. In addition, the model estimates the mass flow rate, the compressor power input and the discharge temperature with a deviation lower than ±2%, ±3%, and ±4 K, respectively. The compressor efficiency of each compressor stage is calculated by Equation (7) and the volumetric efficiency is calculated by Equation (6). Moreover, the overall compressor efficiency of the TSRC is calculated by Equation (11).

The swept volumes of the two-stage compressors are defined to have the same heating capacity as the SCVI in the nominal operating conditions. The nominal operating conditions are $T_e$=-15 °C, $T_c$=50 °C, SH=5 K, SC=5 K, $SH_{inj}$=5 K. The cycle has an economizer in the injection mechanism ($\Delta T_{6\text{-}7}$=5 K). The cycle parameters are SH=10 K, $SH_{inj}$=5 K, SC=5 K. The thermophysical properties of the refrigerant at the different points are calculated with the NIST REFPROP database [16]. All the models have been implemented using EES software [17].

## 2.2 Experimental test bench

Figure 5 illustrates the scheme of the calorimetric test bench used for testing the compressors. The installation has an additional injection line (gray line in Figure 5) for testing the SCVI, as described by [7]. The refrigerant conditions at compressor inlet (pressure and temperature) and outlet (pressure) are adjusted with PID control loops. The condensing pressure, evaporating pressure and the superheat at the compressor inlet are set acting on the flow rate of the water condenser, valves EEV-2, and resistors of the calorimeter, respectively. To test the SCVI, the injection line is enabled by opening the ball valve V-1. The electronic expansion valve EEV-1 regulates the intermediate pressure. The injection superheat is fixed with the water-glycol temperature through a heat exchanger. Electric resistors control the temperature of the water-glycol mixture in order to fix the injection superheat. To test the non-injected scroll compressor (SCNI) and the reciprocating compressor (RC), the injection line is disabled by closing the ball valve V-1. The test bench is equipped with instruments for measuring the pressure and temperature in the suction, discharge and injection of the compressor (points 1, 8 and inj in Figure 5). The instrument accuracies of pressure transmitter (Fisher–Rosemount 3051) and temperature transmitter (RTD-PT 100) are 0.02 % and 0.05 ºC, respectively.

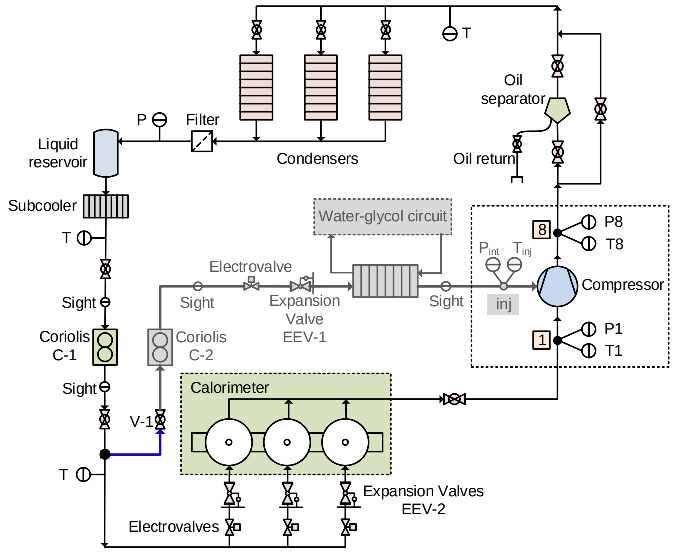


Figure 5. Scheme of the calorimetric test bench.

The refrigerant mass flow rate is measured based on the European Standard EN 13771-1 [18]. Primary and confirming measurements were conducted simultaneously. The primary test procedure is the secondary refrigerant calorimeter method and the confirming test method is a Coriolis-type mass flow meter. The mass flow rate through the condenser was measured after the subcooler by using a Coriolis-type (Fisher–Rosemount Micro-Motion CMF025M), C-1 in Figure 5. The injection mass flow rate was measured with a Coriolis-type mass flow meter with uncertainty of ±0.025 g $s^{-1}$ (C-2). The evaporator mass flow rate is calculated as the difference between the condenser mass flow rate and the injection mass flow rate and is compared with the secondary refrigerant calorimeter based result. The compressor power input was measured with an electrical power meter with a precision of 0.1%.

The swept volumes of the compressors are 17.28 $m^3h^{-1}$ for the SCVI, 17.49 $m^3h^{-1}$ for the SCNI and 20.71 $m^3h^{-1}$ for the RC. All the compressors were tested with R-290 as refrigerant. For the SCVI, the laboratory tests were performed according to the following parameters: suction superheat of 10 K, injection superheat of 5 K, and subcooling at the condenser outlet of 5 K. For the SCNI and the RC, the parameters used were suction superheat of 10 K and subcooling at the condenser outlet of 5 K. The test points were selected as a function of the compressor working envelope of the manufacturer and considering operating conditions for heating applications. Figure 6 shows the working map of the compressors and the tested points for each compressor.

a) b)

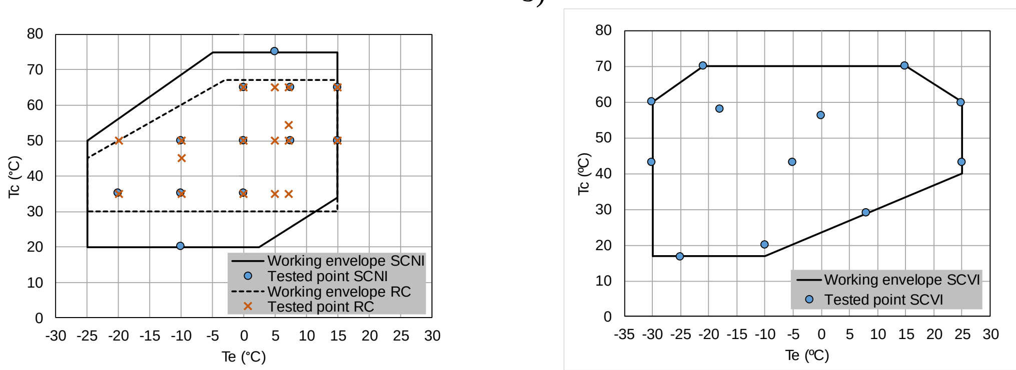


Figure 6. Compressor working envelope and test points for the compressors working with R-290. a) SCNI and RC. b) SCVI.

## 3. Results and discussion

Figure 7 shows the compressor efficiencies of the three compressors tested in the calorimetric test bench. The experimental compressor efficiencies are plotted as a function of the pressure ratio. The experimental data of the tested compressors are used to fit the parameters of the compressor models. Table 1 summarizes the parameters of the compressor models.

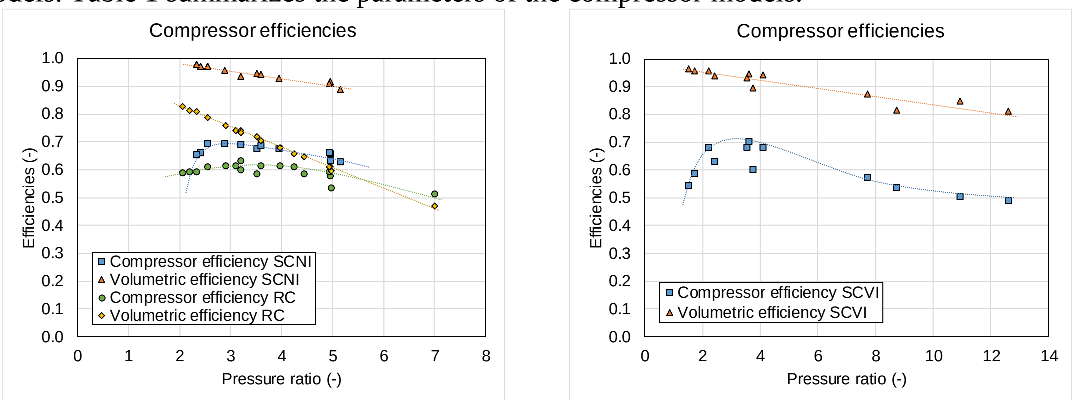


Figure 7. Experimental efficiencies of the compressors. a) SCNI and RC. b) SCVI. Refrigerant R-290.

Table 1 – Model parameters fitted from the experimental data of the compressors.

| Comp. | Parameters | | | | | | | | | | |
|---|---|---|---|---|---|---|---|---|---|---|---|
| | $\varepsilon$ (-) | $K_1$ ($K^{-1}$) | $K_2$ ($m^{1/5}$) | $K_3$ ($m^{-4}$) | $K_4$ ($m^{-4}$) | $K_5$ (-) | $K_6$ (J s) | $\eta_{el}$ (-) | $UA_{amb}$ (W $K^{-1}$) | $A_{leak}$ ($m^2$) | $K_v$ (-) |
| **SCNI** | 2.9 | 0.928 | 0.085 | 1.37E+6 | 2.21E+8 | 70.68 | 127 | 0.88 | 0.55 | 1.15E-5 | - |
| **RC** | - | 0.9 | 0.902 | 3.83E+8 | 3.18E+9 | 69.34 | 232 | 0.859 | 0.75 | 1.08E-4 | 0.055 |
| **SCVI** | 2.98 | 0.92 | 0.08 | 4.06E+6 | 8.71E+8 | 54.57 | 335 | 0.864 | 0.81 | 8.53E-6 | - |

Once the compressor models were adjusted, they can be used to simulate the performance of the SCVI and each compression stage of the TSRC and the TSSC. In the case of the SCVI the parameters of the Equation (10) are also fitted by linear regression, A=-0.593, B=0.474 with an R-square factor higher than 0.99. The swept volume of the TSSC is 17.49/10.15 $m^3h^{-1}$ and for the

TSRC is 20.71/11.78 $m^3h^{-1}$. The performance of the three compressors is calculated for several operating conditions, considering heat pump applications working with high pressure ratios. These applications include heat pumps operating in cold regions (low evaporating temperatures), and heat pumps operating with high condensing temperatures such as high-temperature water heating applications and radiator heating systems. The evaporating temperatures considered were from -30 °C to 20 °C, and the condensing temperatures considered were from 40 °C to 80 °C.

### 3.1 Comparison of the compressor efficiencies

Figure 8a depicts the overall compressor efficiency as a function of the pressure ratio. The studied operating conditions correspond to pressure ratios greater than 3. Under these conditions, the SCVI is working outside the optimum efficiency. The optimum efficiency of the SCVI could be achieved for pressure ratios around 3 (see Figure 7b), nevertheless, for higher pressure ratios the efficiency decreases rapidly due to the effects of under-compression, as shown in Figure 8a.

The optimum efficiencies of the TSRC and TSSC are found for pressure ratios around 5.5 and 7.5, respectively. For higher pressure ratios, the efficiencies decrease smoothly, getting to work with a wide range of pressures. The efficiency curves of the two-stage compressors (TSRC and TSSC) have less slope than that of the SCVI. This is owed to the differences in the compression process. The SCVI works with a higher pressure ratio than each stage compressors of the TSRC and the TSSC. The SCVI compress from the evaporating pressure to the condensing pressure. Nevertheless, in the two-stage compressors, each compression stage works with a lower compression ratio. Hence, they are working closer to their optimum efficiency. The SCVI improves the efficiency for pressure ratios up to 4.5 and 6.5 compared with the TSSC and TSRC, respectively. The TSSC improves the efficiency for all the studied range of pressures compared with the TSRC and improves the efficiency for pressure ratios from 4.5 compared with the SCVI.

a) b)

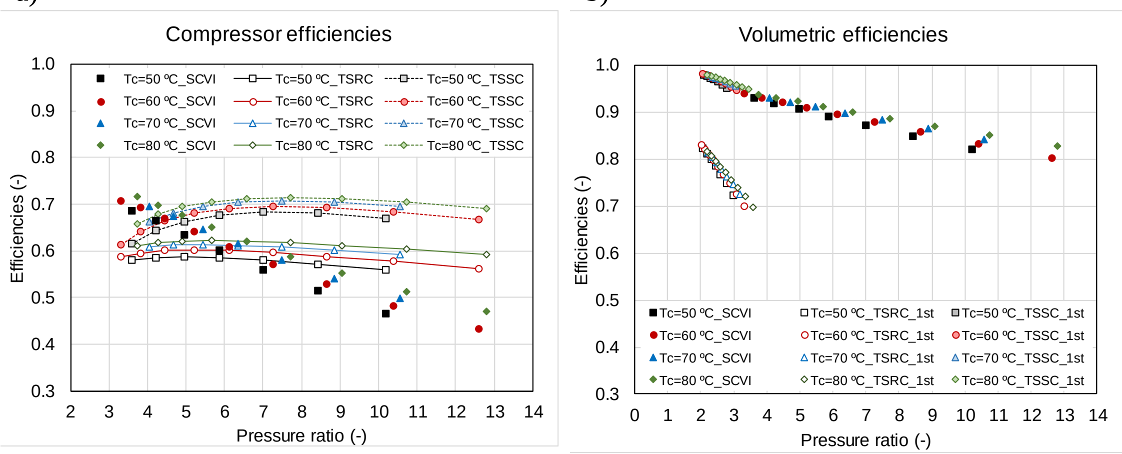


Figure 8. a) Compressor efficiency as a function of pressure ratio. b) Volumetric efficiencies as a function of pressure ratio at several condensing temperatures.

Figure 8b depicts the volumetric efficiency as a function of the pressure ratio. For comparison purposes, the represented curves for the two-stage compressors correspond to the first stage of compression, since the volumetric efficiency is related to the evaporator mass flow rate. The SCVI and TSSC present curves of volumetric efficiency with less slope. These scroll compressors present high volumetric efficiency, above 0.8 for any operating point. This is owed to the absence of re-expansion volumes, the continuous-flow process, and the good axial and radial compliance of the scroll members. The TSRC presents volumetric efficiency curves with a higher slope. For the first stage of compression, the volumetric efficiency drops to 0.7 for a pressure ratio of 3.3.

## 3.2 Comparison of the heating capacity

Figure 9a illustrates the heating capacity as a function of the evaporating temperature. The heating capacities of the compressors are similar since the compressor size of the two-stage compressors were optimized to have the same heating capacity than the SCVI at the nominal point. Nevertheless, the SCVI presents curves of capacity with less slope compared with the curves of the two-stage compressors. The heating capacity of the SCVI is slightly higher for low evaporating temperatures (less than 0 °C); this is owed to the differences in the volumetric efficiency of the compressors shown in Figure 8b, and because the SCVI has a larger injection ratio, as shown in Figure 9b. For higher evaporating temperatures, like 20 °C, the TSRC improves the heating capacity by 1.5% and 3.6% compared with TSSC and SCVI, respectively (condensing at 80 °C).

The differences in the injection ratio of the three compressor technologies are owed to the SCVI compresses the refrigerant in a single stage with refrigerant injection at an intermediate point during the compression. The amount of injected refrigerant depends on the location and size of the injection ports. While the two-stage compressors have two well-defined stages of compression in separated pistons or scrolls, and the amount of injected refrigerant depends on the size of the high stage compressor.

a) b)

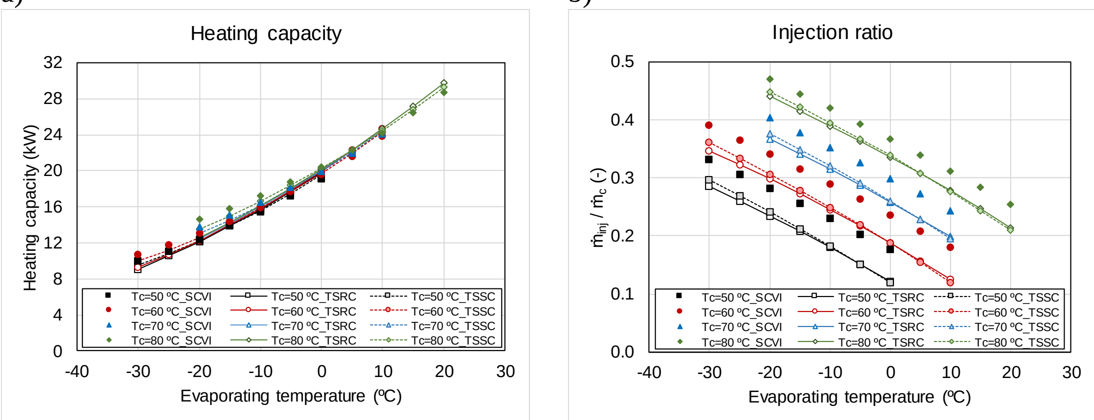


Figure 9. a) Heating capacity as a function of evaporating temperature. b) Injection ratio as a function of evaporating temperature at several condensing temperatures.

## 3.3 Comparison of the heating COP

Figure 10 illustrates the heating COP according to the evaporating temperature. The system with SCVI presents curves of COP with a higher slope. Therefore, the SCVI improves the COP compared with the TSSC for working conditions corresponding to pressure ratios above 5. This is due to the higher compressor efficiency of the SCVI in these conditions (see Figure 8a) and the differences in the injection ratio (see Figure 9b).

The systems with two-stage compressors present curves with less slope, which implies a better performance when the compressors work with lower evaporating temperatures. Nevertheless, the TSSC improves the COP in all working conditions compared with TSRC, mainly owed to the higher compressor efficiency of the TSSC (see Figure 8a). For pressure ratios above 7.5, the TSSC presents a better COP than the other two compressors. For example, at the point (-20 °C, 50 °C), the system with TSSC improves the COP by 11.3% and 12.5% compared with SCVI and TSRC, respectively. For higher condensing temperatures, such as 80 °C, the COP of the TSSC is improved by 19.7% and 9.4% compared with SCVI and TSRC, respectively. In the same point (-20 °C, 50 °C), the system with SCVI improves the COP by 1.1% compared with TSRC, but for higher condensing temperatures, such as 80 °C, the COP is lower than TSRC by 9.5%. This difference in COP is owed to the SCVI efficiency decreases for pressure ratios higher than 6.5. When the compressors work with higher evaporating temperatures like 0 °C (pressure ratios below 7), the system with SCVI improves the COP up to 11.6% and 17.7% compared with TSSC and TSRC, respectively (condensing at 50 °C). However, for higher condensing temperatures, such as 80 °C, the system with TSSC improves the COP by 7.1% and 9.9% compared with SCVI and TSRC, respectively. The results suggest that the SCVI can be used in heat pumps and air conditioning systems working under moderate temperature conditions and pressure ratios below 6.5; the TSRC can be used in water heating systems in cold climates and high pressure ratios (above 6.5). The TSSC can be used in water heating systems in cold climates but under a wider range of pressure ratios (above 4.5).

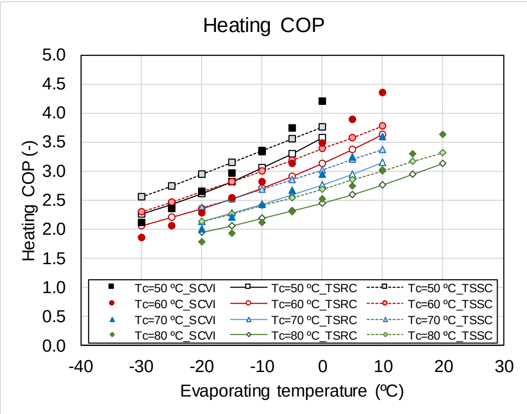


Figure 10. Heating COP as a function of the evaporating temperature at several condensing temperatures.

## 3.4 Comparison of the discharge temperature

Figure 11a shows the discharge temperature of the compressors as a function of the evaporating temperature. The discharge temperature curves of the two-stage compressors have less slope than the curves of the SCVI. This means that the two-stage compressors can extend more the working map for lower evaporating temperatures than the SCVI.

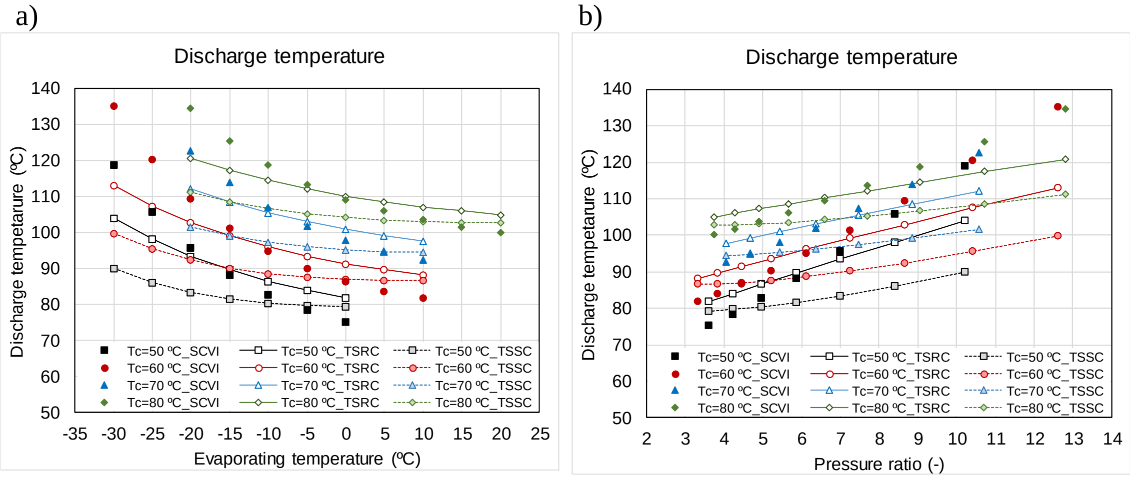


Figure 11. a) Discharge temperature as a function of the evaporating temperature. b) Discharge temperature as a function of the pressure ratio at several condensing temperatures.

Comparing the SCVI with the two-stage compressors, Figure 11b shows that the SCVI achieves a lower discharge temperature than the TSSC for low pressure ratios (below 4.8). For pressure ratios lower than 7, the SCVI achieves lower discharge temperatures than the TSRC. Regarding the two-stage compressors, the TSSC achieves a lower discharge temperature than the TSRC for all the working conditions considered in the study. This is owed to the higher compressor efficiency of the TSSC. For extreme conditions ($P_r$>4.8), the TSSC presents a lower discharge temperature than the SCVI.

If the discharge temperature is limited to 120 °C, taking into account the possible degradation of the lubricating oil, the working map of the SCVI is more restricted than that of the two-stage compressors. The SCVI could work evaporating up to -30 °C, -25 °C, -18 °C and -12 °C, condensing at 50 °C, 60 °C, 70 °C and 80 °C, respectively. This corresponds to compression ratios less than 10.5 for condensing temperatures between 50 °C and 70 °C, and compression ratios less than 9.5 for a condensing temperature of 80 °C. Since the curves of the two-stage compressors have less slope, they can work in a wider range of working conditions. However, for very high condensation temperatures (80 ºC), the TSRC could work evaporating up to -18 ºC ($P_r$=12.5).

The differences in the discharge temperature between the SCVI and the two-stage compressors is due to the fact that the compression in the SCVI is more like compression in one stage, while in the other compressors there are well-defined compression stages. This leads us to think that the two-stage compression with vapor-injection, independently of the compressor technology, is more effective in the reduction of the discharge temperature than the vapor-injection compressors (SCVI). Therefore, two-stage compressors can be used in applications such as high-temperature water heating up to 80 °C.

## 4. Conclusions

A comparative analysis of the compressor performance of a vapor-injection scroll compressor (SCVI) and a two-stage scroll compressor (TSSC) working with high-pressure ratios is presented. The analysis was performed in terms of compressor efficiencies, heating capacity, COP, and discharge temperature, using R-290 as refrigerant. In addition, a two-stage reciprocating compressor (TSRC) was included in the study, as an alternative compressor technology available in the market for heat pump applications. The following conclusions can be drawn from the study:

- The SCVI advantage is the easy implementation of vapor-injection from the machining point of view. Instead, the disadvantage of the SCVI is that over- and under-compression easily occurs when the operating conditions deviate from the specified designed condition due to the fixed built-in volume ratio determined by the scroll geometry. Hence, SCVI could not achieve the optimum when the operation conditions differ from the design compression ratio.
- The SCVI presents better compressor efficiency for pressure ratios up to 4.5. For higher-pressure ratios, the TSSC presents better compressor efficiency than SCVI and TSRC.
- Across the working range, the SCVI and TSSC present better volumetric efficiency than the TSRC, and the relative difference increases as pressure ratio increases.
- The system with SCVI presents better COP for pressure ratios below 5 due to the higher compressor efficiency in such conditions. For higher pressure ratios, the TSSC presents a better COP than the other two compressors. Nevertheless, the TSRC presents better COP than SCVI for pressure ratios higher than 7.5.
- Regarding the two-stage compressors, the TSSC achieves a lower discharge temperature than the TSRC for all the working conditions considered in the study. The SCVI achieves a lower discharge temperature than the TSSC for low compression ratios (lower than 4.8), and a lower discharge temperature than the TSRC for compression ratios below 7.

## 5. Acknowledgements

Fernando M. Tello-Oquendo acknowledges the financial support provided by the CONVOCATORIA ABIERTA 2013-SEGUNDA FASE program, which was funded by the SENESCYT (Secretaría de Educación Superior, Ciencia, Tecnología e Innovación) (Grant No 2015-AR37665) of Ecuador. The authors acknowledge the Spanish "MINISTERIO DE ECONOMIA Y COMPETITIVIDAD", through the project ref-ENE2017-83665-C2-1-P "Maximización de la eficiencia y minimización del impacto ambiental de bombas de calor para la descarbonización de la calefacción/ACS en los edificios de consumo casi nulo" for the given support.

## 6. References

[1] Xu, X., Hwang, Y. and Radermacher, R. *Refrigerant injection for heat pumping/air conditioning systems: literature review and challenges discussions*. International Journal of Refrigeration, 2011, vol. 34, pp. 402-415.

[2] Wang, X., Hwang, Y. and Radermacher, R. *Two-stage heat pump system with vapor-injected scroll compressor using R410A as a refrigerant*. International Journal of Refrigeration, 2009, vol. 32, pp. 1442-1451.

[3] Wang, B., Shi, W., Han, L., Li, X. *Optimization of refrigeration system with gas-injected scroll compressor*. International Journal of Refrigeration, 2009, vol. 32, pp. 1544-1554.

[4] Feng, C., Kai, W., Shouguo, W., Ziwen, X., Pengcheng, S. *Investigation of the heat pump water heater using economizer vapor injection system and mixture of R22/R600a*. International Journal of Refrigeration, 2009, vol. 32, pp. 509-514.

[5] Xu, S., Ma, G., Liu, Q., Liu, Z. *Experiment study of an enhanced vapor injection refrigeration/heat pump system using R32*. International Journal of Thermal Sciences, 2013, vol. 68, pp. 103-109.

[6] Navarro, E., Redón, A., Gonzálvez, J., Martinez, I. *Characterization of a vapor injection scroll compressor as a function of low, intermediate and high pressures and temperature conditions*. International Journal of Refrigeration, 2013, vol. 36, pp. 1821- 1829.

[7] Tello-Oquendo, F.M., Navarro-Peris, E., Gonzálvez-Maciá, J. *New characterization methodology for vapor-injection scroll compressors*. International Journal of Refrigeration, 2017, vol. 74, pp. 526-537.

[8] Winandy, E.L., Lebrun, J. *Scroll compressors using gas and liquid injection: experimental analysis and modelling*. International Journal of Refrigeration, 2002, vol. 25, pp. 1143-1156.

[9] Tello-Oquendo, F.M., Navarro-Peris, E., Gonzálvez-Maciá, J. *Performance of a scroll compressor with vapor-injection and two-stage reciprocating compressor operating under extreme conditions*. International Journal of Refrigeration, 2016, vol. 63, pp. 144-156.

[10] Kwon, O., Cha, D. and Park, C. *Performance evaluation of a two-stage compression heat pump system for district heating using waste energy*. Energy, 2013, vol. 57, pp. 375-381.

[11] Bertsch, S.S., Groll, E.A. *Two-stage air-source heat pump for residential heating and cooling applications in northern U.S. climates*. International Journal of Refrigeration, 2008, vol. 31, pp. 1282-1292.

[12] Tello-Oquendo, F.M., Navarro-Peris, E., Gonzálvez-Maciá, J. *Comparison of the compressor losses of a scroll and a reciprocating compressor working with propane*. 13th IIR Gustav Lorentzen Conference. Valencia-Spain, 2018, Paper 1269.

[13] Tello-Oquendo, F.M., Navarro-Peris, E., Barceló, R., Gonzálvez-Maciá, J. *Semi-empirical model of scroll compressor and its extension to describe vapor-injection compressors. Model description and experimental validation*. International Journal of Refrigeration, 2018, submitted.

[14] Navarro, E., Granryd, E., Urchueguía, J.F., Corberán, J.M. *A phenomenological model for analyzing reciprocating compressors*. International Journal of Refrigeration, 2007, vol. 30, pp. 1254-1265.

[15] Navarro, E., Urchueguía, J.F., Corberán, J.M., Granryd, E. *Performance analysis of a series of hermetic reciprocating compressors working with R290 (propane) and R407C*. International Journal of Refrigeration, 2007, vol. 30, pp. 1244-1253.

[16] Lemmon, E., Huber, M., Mc Linden, M. NIST Standard Reference Database 23: Reference Fluid Thermodynamic and Transport Properties-refprop. Version 9.0. Gaithersburg: National Institute of Standards and Technology, Standard Reference Data Program, 2010.

[17] Klein, S.A., Alvarado, F.L. EES-Engineering Equation Solver. Academic Professional Version 10.091. F-Chart Software. Madison, WI. 2017.

[18] EN 13771-1. Compressors and condensing units for refrigeration - Performance testing and test methods - Part 1: Refrigerant compressors. Brussels, Belgium: EN Standard: European Committee for Standardization, 2016.